

Strong water isotopic anomalies in the martian atmosphere: Probing current and ancient reservoirs

G. L. Villanueva,^{1,2*} M. J. Mumma,¹ R. E. Novak,³ H. U. Käufl,⁴ P. Hartogh,⁵ T. Encrenaz,⁶ A. Tokunaga,⁷ A. Khayat,⁷ M. D. Smith

¹NASA Goddard Space Flight Center, Greenbelt, MD 20771, USA. ²Catholic University of America, Washington, DC 20064, USA. ³Iona College, New Rochelle, NY 10801, USA. ⁴European Southern Observatory, Munich, Germany. ⁵Max Planck Institute for Solar System Research, Katlenburg-Lindau 37191, Germany. ⁶Observatoire de Paris-Meudon, Meudon 92195, France. ⁷University of Hawaii-Manoa, Honolulu, HI 96822, USA.

*Corresponding author. E-mail: geronimo.villanueva@nasa.gov

We measured maps of atmospheric water (H_2O) and its deuterated form (HDO) across the martian globe, showing strong isotopic anomalies and a significant high D/H enrichment indicative of great water loss. The maps sample the evolution of sublimation from the north polar cap, revealing that the released water has a representative D/H value enriched by a factor of about 7 relative to Earth's ocean (VSMOW). Certain basins and orographic depressions show even higher enrichment, while high altitude regions show much lower values (1 to 3 VSMOW). Our atmospheric maps indicate that water ice in the polar reservoirs is enriched in deuterium to at least 8 VSMOW, which would mean that early Mars (4.5 billion years ago) had a global equivalent water layer at least 137 meters deep.

We report maps of water isotopologues (H_2O and its deuterated form HDO) across the martian globe, which show strong isotopic anomalies that are difficult to reconcile with simple fractionation processes. These maps address fundamental unknowns such as the current representative ratio of D/H in water and how much water was lost over the geological life of the planet. Isotopic ratios are among the most valuable indicators for the loss of volatiles from an atmosphere. Deuterium fractionation also reveals information about the cycle of water on the planet and informs us of its stability on short- and long-term scales. The vapor pressures of HDO and H_2O differ substantially near the freezing point, making the condensation/sublimation cycle of the isotopologues sensitive to local temperatures and saturation levels and to the presence of aerosol condensation nuclei.

Although many maps of H_2O do exist [e.g., (1, 2)], and some of HDO [e.g., (3, 4)], 2-D maps of atmospheric D/H enrichment on Mars do not. Apart from preliminary 2-D maps presented at conferences (5), previous mapping attempts to measure D/H provided only 1-D maps of HDO and H_2O based on nearly-simultaneous measurements at ground-based IR observatories [e.g., (6–9)] or 1-D HDO maps (ground-based) and quasi-simultaneous H_2O measurements taken from Mars orbit via PFS/LW (10). Local isotopic ratios such as derived by Curiosity/MSL (11) are representative of that specific location and time, and may not represent the actual D/H of atmospheric water on Mars

(see more below), even though reports of hemispherically averaged D/H in water indicated a similar value of 5–6 times the D/H of Earth's oceans (VSMOW) (12, 13). Importantly, such isolated (in time and in space) measurements of D/H in the atmosphere were typically – but incorrectly – assumed to be representative of the bulk atmosphere. Spatially resolved measurements of D/H at different times of day and seasons are necessary to disentangle local from global phenomena. Such maps reveal the true isotopic ratio of current water reservoirs with implications for the global loss of water over geologic time, and may also assist in the identification of new sources of water on Mars.

Currently, the martian atmosphere and surface form an arid and highly inhospitable environment (14, 15). The upper layers of soil were heavily eroded

by long-term aeolian activity, and soil chemistry was strongly modified through exposure to energetic photons and particles that penetrated owing to inadequate magnetospheric and atmospheric shielding. However, there is ample evidence that ancient Mars was wet and likely hosted habitable conditions (16, 17). Particularly during the Noachian age (3.6 – 4.5 billion years ago), probably leading to the formation of rich subsurface aqueous reservoirs. Moreover, the presence of extensive volcanism likely gave rise to widespread hydrothermal activity and to the formation of diverse chemical environments. Measurements of epithermal neutron fluxes obtained by Mars Odyssey (18) suggest the presence of important near-surface hydrogen concentrations on Mars, and the Polar Layered Deposits (PLD) are estimated to contain ~21 m global equivalent layer (GEL) of water (19, 20). The atmosphere acts as a buffer between the exosphere (at the boundary with outer space) and the main reservoirs of H, C and O (e.g., regolith and polar caps), with atmospheric isotopic/abundance ratios providing key diagnostics for quantifying the exchange among these environments.

The maps reported herein are based on observations of isotopic water made with high-resolution spectrometers [CRIRES (cryogenic infrared echelle spectrograph), NIRSPEC (near infrared spectrograph), CSHELL (cryogenic echelle spectrograph)] at powerful ground-based observatories [VLT (Very Large Telescope), Keck, and IRTF (InfraRed Telescope Facility), respectively] (SM-1). This program is

founded on initial observations performed using NASA's Kuiper Airborne Observatory and the Kitt Peak National Observatory in 1989 (13), and later with IRTF (6, 7). Specifically we targeted the ν_1 band of HDO near 2720 cm^{-1} ($3.7\text{ }\mu\text{m}$), and the $2\nu_2$ band of H_2O near 2990 cm^{-1} ($3.3\text{ }\mu\text{m}$) (see Fig. 1). Spectral lines of these bands on Mars are observable through our atmosphere when measured from high-altitude observatories at moderately high Doppler shifts ($>11\text{ km s}^{-1}$), i.e., when Mars' lines are displaced sufficiently far from the cores of their counterpart telluric absorbing lines. Observations of HDO are additionally favored by the large D/H enrichment present in the martian atmosphere and the strong D/H depletion in terrestrial air at the high-altitudes of these observatories (9) which leads to high telluric transmittances. We obtained greatest sensitivities to HDO and H_2O on Mars by performing observations at times of maximum Doppler-shifts, typically several months before or after Mars closest approach to Earth (every ~2 years).

Mapping was achieved by stepping the spectrometer's entrance slit across the planet and sampling the planet's spectrum at intervals along the slit for each step, leading to full two-dimensional (E-W and N-S) coverage across the observable disk (see details in SM-1). The distance between slit positions was set in accord with observational image quality ("seeing"), guiding precision, and slit width. For a typical Mars diameter of $8''$, a slit-width of $0.2''$ and a "seeing" of $0.6''$, a typical map would consist of 11 slit positions stepped across the planet, with a minimum of 9 positions for less favorable conditions. For each slit position, abundance measurements are obtained at intervals of $0.6'$ along the slit. The maps are of relatively high spatial resolution (~500 km near sub-earth positions), and importantly, each map was obtained within a short time interval (1-2 hours), thereby providing hemi-global snapshots in time that are critical for investigating the effects of local phenomena (e.g., orographic clouds, planet-scale waves) and transient processes (e.g., polar releases and diurnal effects).

The data reported herein were collected over several years and seasons on Mars from March 2008 until January 2014. From this database, we made a localized D/H measurement over the Viking 1 landing site (9) and obtained a comprehensive search for organics in the martian atmosphere (15). Here, we present results from the best datasets targeting D/H, obtained at times of low telluric water, high-Doppler shift and maximum spatial coverage (CRIRES: September/8-9/2009, CSHELL: March/25/2008, NIRSPEC: January/24/2014, CRIRES: January/29-30/2014) (see Fig. 2 and fig. S1). The data spans seasons from late northern winter to late northern spring on Mars (areocentric longitude or season $L_s = 335^\circ, 50^\circ, 80^\circ, 83^\circ$), and samples the critical interval when the northern polar cap sublimates and replenishes the atmosphere with water.

The highest spectral resolution is achieved with the narrow slit ($0.2''$) of CRIRES leading to a resolving power of $\lambda/\delta\lambda \sim 100,000$, while the cross-dispersed feature of

NIRSPEC provides the broadest spectral coverage at a high resolving power of $\lambda/\delta\lambda \sim 40,000$. Such broad spectral coverage allows us to sample HDO and H_2O with a single NIRSPEC setting, while measurements with CRIRES and CSHELL require mappings at two spectral settings ($3.7\text{ }\mu\text{m}$ and $3.3\text{ }\mu\text{m}$). Each setting also samples lines of CO_2 that we use to establish the total atmospheric column and to quantify extinction and scattering effects by water ice and dust aerosols (SM-2). Abundance ratios and column densities for H_2O and HDO at each footprint are then corrected for local (spatial and spectral) variations in the co-measured CO_2 column, removing an important source of systematic error that would otherwise affect isotopic measurements. We derive molecular column densities at each footprint by comparing the residual spectrum to a synthetic Mars spectrum (color traces in Fig. 1), itself affected by the monochromatic telluric transmittance for each spectral line at its Mars Doppler-shifted spectral position. For this process, we employ the efficient and robust Levenberg-Marquardt curve-fitting method, which also provides reliable error estimates as derived from the measured Jacobians (SOM-1). We typically obtain high signal-to-ratios (SNR) of ~70 for the HDO columns with CRIRES, but the precision of the D/H ratio is defined mainly by the H_2O columns. The median accuracy of the D/H measurements is 0.2, 0.5, 0.8 and 0.4 VSMOW for the Jan/2014 (CRIRES), Jan/2014 (NIRSPEC), Sep/2009 (CRIRES) and Mar/2008 (CSHELL) observations respectively.

The H_2O and HDO disk maps (Fig. 2) reveal strong local anisotropies and seasonal variability. The slow replenishing of water vapor in the northern hemisphere as the polar cap sublimates during northern spring is quite noticeable, in particular when compared to the baseline measurement in late northern winter ($L_s 335^\circ$). Variability of H_2O with latitude and season is apparent (Fig. 2), and is generally consistent with previous spacecraft measurements of the water cycle (21, 22). HDO maps superficially resemble those of H_2O in showing strong variability, but their direct comparison reveals strong differences that are most easily seen in the maps of the ratio of D/H enrichment in water vapor, relative to Earth's oceans [VSMOW (Vienna Standard Mean Ocean Water)].

The maps of D/H enrichment show a remarkably different evolution and structure compared with total water, with an apparent relationship to topography and atmospheric temperature. Low D/H values are seen at high altitudes while high D/H values are seen in basins and orographic depressions. Very low D/H [1-3 VSMOW] appears in the winter hemisphere, but the spring hemisphere shows much higher values. The Vapor Pressure Isotope Effect (VPIE), which produces an isotopic fractionation at condensation (e.g., cloud formation and frost/ground fog formation), could explain some of this latitudinal variability, yet the observed localized (in time and space) anisotropies are certainly higher than was predicted by current atmospheric

models (23, 24). For instance, preferential condensation of HDO could perhaps explain the strong D/H depletion seen in clouds over Elysium Mons on Jan/24/2014, and similarly over the Tharsis district as observed in Sep/2009 and Jan/2014. Interestingly strong clouds are observed over this region by the MARCI camera onboard MRO (25). As discussed in (24), Rayleigh distillation would provide the strongest isotopic fractionation, yet on Mars competition between condensation and sedimentation may lead to certain non-equilibrium fractions, while kinetic processes may enhance or diminish the efficiency of fractionations on Mars as is observed on Earth (26).

Importantly, our maps reveal notably higher deuterium enrichment than was found in globally averaged observations that indicated $D/H = 5.0 \pm 0.2$ VSMOW (13) and 5.8 ± 2.6 VSMOW (12). This difference is expected because full disk measurements reflect the mean of diverse regions with high and low D/H revealed by our maps (Fig. 2). Moreover, isolated measurements from a discrete region may reflect local climatological effects, and so may not represent the deuterium enrichment of the bulk atmosphere. For instance, Gale Crater (location of the MSL Curiosity rover) is at the boundary of a strong gradient between two regions of D/H that range from 1 to 7 VSMOW, where local and seasonal effects may affect retrievals of D/H (L_s 50, Fig. 2). Our value at Gale Crater (6 VSMOW; L_s 50 and 80) is in good agreement with that derived with the MSL-TLS instrument (6 ± 1 VSMOW) in late 2012 (11). However, our maps reveal that in regions and seasons where both isotopologues are expected to be fully gaseous (equatorial and mid-latitudes during mid- and late-spring, L_s 50, 83, 80) the atmosphere shows high D/H (~7 VSMOW), with some regions showing strong enrichments reaching 9–10 VSMOW.

Temperature is the main parameter governing isotopic ratios in an atmosphere, but other factors such as relative humidity (condensation level), presence of dust particles (condensation nuclei), and dynamical / transport processes (e.g., expansive cooling due to vertical lifting) affect the rate at which condensation occurs for each isotopologue. These factors impact the observable gas phase D/H ratio (see D/H correlations with temperature and water column in SM-3). Models for the seasonal behavior of the D/H ratio on Mars incorporate some of these effects. Using a 3D general circulation model that included fractionation effects, Montmessin *et al.* (24) predicted hemispheric variability with a peak atmospheric D/H value 15% lower than the value assumed for the polar caps. In general, our results are in agreement with the predicted level of variability with latitude, but the strong local anisotropies observed across the planet will require a more realistic model to account for several climatological processes acting on the isotopologues. Importantly, our typical atmospheric value (7 VSMOW) implies that the permanent polar caps contain a D/H of 8 VSMOW, following the modeling results in (24).

The great obliquity variations experienced by Mars at

million year intervals (27) should have caused all major ice reservoirs to vaporize and re-form repeatedly, causing refreshed mixing of water from the different repositories at regular intervals. If so, all near-surface and polar reservoirs of water on Mars should share a relatively common D/H ratio. Since we also observe even higher D/H values (above 8 VSMOW) in certain regions, such mixing would suggest that the current reservoirs of water on Mars contain a higher D/H than initially thought, and would consequently require greater loss of water over the planet's lifetime.

Multiple reservoirs have been proposed to account for the current inventory of water on Mars, ranging from the observable polar layered deposits (PLD) (19, 20), to ice-rich regolith at mid-latitudes (28, 29), near-surface reservoirs at high-latitudes (30), and sub-surface reservoirs as implied by gamma ray and neutron observations (31). As nicely summarized by Kurokawa *et al.* (32), the PLD can be defined as the minimum estimate of the current inventory of Mars. The PLD would correspond to $1.4 \pm 0.3 \times 10^{18}$ kg of water [or 10 ± 2 m GEL of water for the North polar region (19)] and $1.6 \pm 0.2 \times 10^{18}$ kg (11 ± 1.4 m GEL) for the South polar region (20), totaling 21 ± 3.4 m for the PLD reservoir. Recent estimates suggest the PLDs contain 17–21 m GEL, with 25–29 m GEL across all directly measured reservoirs (33). The initial reservoir of water on Mars (M_p) can be estimated from the current inventory of water on Mars (M_c) and its isotopic ratio (I_c) when knowledge of the ancient isotopic ratio (I_p) exists, together with the fractionation escape rate (f) of the isotopologues, using the relation equation: $M_p/M_c = (I_c/I_p)^{[1/(1-f)]}$. From HST measurements of D and H Lyman-alpha emission in the upper atmosphere of Mars, Krasnopolsky *et al.* (34), derived a fractionation rate of 0.02. Usui *et al.* (35) measured a water D/H of 1.275 VSMOW in melt inclusions (estimated to be 4.5 Ga old) within the Mars meteorite Yamato 980459. Taking this value as I_p , 21 m GEL as M_c , our estimate of 8 VSMOW (for the PLD) as I_c implies that Mars had at least 137 m GEL of water 4.5 Ga ago (see Fig. 3).

This value could be defined as a lower bound for the original GEL because it is based on the minimum current water reservoir (PLD) and neglects the young Sun's high EUV fluxes (36), that would have lead to unfractionated escape of H and D. If we assume that all currently measured water reservoirs (25–29 m), including the atmosphere, share the representative 7 VSMOW enrichment, then the ancient estimate is 142–165 m, further establishing the 137 m GEL value as a lower bound. Considering Mars' current topography (37), 137 m GEL water would have covered up to 20% of the planet's surface (38). Meteoritic records dated to 4.1 Ga (39, 40) and clay minerals in Gale Crater (41) indicate a much higher D/H than in Yamato 980459, implying that the loss of water from Mars occurred in stages (32), with a substantial amount of water being lost in the first 0.5 Ga. Geomorphological records on Mars do indicate a wetter past (up to >2000 m GEL), yet as summarized by Carr and Head

(38) and more recently confirmed by sub-surface observations with MARSIS (42), the best estimate is provided by the Vastitas Borealis Formation (VBF), which implies 2.3×10^7 km³ of water (156 m GEL). This estimate is in relatively good agreement with our value (137 m GEL) as inferred from our estimate of D/H enrichment (8 VSMOW) in the polar layered deposits. The difference between the two estimates would also mean that ~20 m GEL of water are currently “missing” and could be stored in other proposed water reservoirs (e.g., deep aquifers).

Our D/H maps highlight the importance of obtaining isotopic measurements on Mars that are both spatially and temporally resolved in order to separate climatological from evolutionary effects. Such investigation ultimately leads to a more accurate estimate of the actual D/H of water reservoirs on Mars, and improves both the estimate of water loss over geologic time and estimates for the “missing” water that might reside in undiscovered reservoirs. More realistic estimates on current and ancient fractionation rates [e.g., from NASA’s Mars Atmosphere and Volatile Evolution Mission (MAVEN)] and a larger sample of ancient D/H values derived from authentic (meteorites) and from drilled and/or returned samples would better constrain the water inventory on Mars, current and past.

REFERENCES AND NOTES

- M. D. Smith, Interannual variability in TES atmospheric observations of Mars during 1999–2003. *Icarus* **167**, 148–165 (2004). [doi:10.1016/j.icarus.2003.09.010](https://doi.org/10.1016/j.icarus.2003.09.010)
- M. A. Tschimmel, N. I. Ignatiev, D. V. Titov, E. Lellouch, T. Fouchet, M. Giuranna, V. Formisano, Investigation of water vapor on Mars with PFS/SW of Mars Express. *Icarus* **195**, 557–575 (2008). [doi:10.1016/j.icarus.2008.01.018](https://doi.org/10.1016/j.icarus.2008.01.018)
- R. E. Novak, M. J. Mumma, M. A. Disanti, N. Dello Russo, K. Magee-Sauer, Mapping of ozone and water in the atmosphere of Mars near the 1997 Aphelion. *Icarus* **158**, 14–23 (2002). [doi:10.1006/icar.2002.6863](https://doi.org/10.1006/icar.2002.6863)
- T. Fouchet, R. Moreno, E. Lellouch, V. Formisano, M. Giuranna, F. Montmessin, Interferometric millimeter observations of water vapor on Mars and comparison with Mars Express measurements. *Planet. Space Sci.* **59**, 683–690 (2011). [doi:10.1016/j.pss.2011.01.017](https://doi.org/10.1016/j.pss.2011.01.017)
- G. L. Villanueva et al., Mars Atmosphere: Modeling and Observations Conference, 9101 (2008).
- M. J. Mumma et al., Sixth International Conference on Mars, 3186 (2003).
- R. E. Novak, M. J. Mumma, G. L. Villanueva, B. Bonev, M. A. Disanti, Seventh International Conference on Mars **1353**, 3283 (2007).
- R. E. Novak, M. J. Mumma, G. L. Villanueva, Measurement of the isotopic signatures of water on Mars: Implications for studying methane. *Planet. Space Sci.* **59**, 163–168 (2011). [doi:10.1016/j.pss.2010.06.017](https://doi.org/10.1016/j.pss.2010.06.017)
- G. L. Villanueva, M. J. Mumma, B. P. Bonev, R. E. Novak, R. J. Barber, M. A. DiSanti, Water in planetary and cometary atmospheres: H₂O/HDO transmittance and fluorescence models. *J. Quant. Spectrosc. Radiat. Transf.* **113**, 202–220 (2012). [doi:10.1016/j.jqsrt.2011.11.001](https://doi.org/10.1016/j.jqsrt.2011.11.001)
- S. Aoki et al., European Planetary Science Congress 2013 **8**, EPSC2013 (2013).
- C. R. Webster, P. R. Mahaffy, G. J. Flesch, P. B. Niles, J. H. Jones, L. A. Leshin, S. K. Atreya, J. C. Stern, L. E. Christensen, T. Owen, H. Franz, R. O. Pepin, A. Steele, C. Achilles, C. Agard, J. A. Alves Verdasca, R. Anderson, R. Anderson, D. Archer, C. Armiegos-Aparicio, R. Arvidson, E. Atlaskin, A. Aubrey, B. Baker, M. Baker, T. Balic-Zunic, D. Baratoux, J. Baroukh, B. Barraclough, K. Bean, L. Beegle, A. Behar, J. Bell, S. Bender, M. Benna, J. Bentz, G. Berger, J. Berger, D. Berman, D. Bish, D. F. Blake, J. J. Blanco Avalos, D. Blaney, J. Blank, H. Blau, L. Bleacher, E. Boehm, O. Botta, S. Böttcher, T. Boucher, H. Bower, N. Boyd, B. Boynton, E. Breves, J. Bridges, N. Bridges, W. Brinckerhoff, D. Brinza, T. Bristow, C. Brunet, A. Brunner, W. Brunner, A. Buch, M. Bullock, S. Burmeister, M. Cabane, F. Calef, J. Cameron, J. Campbell, B. Cantor, M. Caplinger, J. Caride Rodríguez, M. Carmosino, I. Carrasco Blázquez, A. Charpentier, S. Chipera, D. Choi, B. Clark, S. Clegg, T. Cleghorn, E. Cloutis, G. Cody, P. Coll, P. Conrad, D. Coscia, A. Cousin, D. Cremer, J. Crisp, A. Cros, F. Cucinotta, C. d'Uston, S. Davis, M. Day, M. de la Torre Juarez, L. DeFlores, D. DeLapp, J. DeMarines, D. DesMarais, W. Dietrich, R. Dingler, C. Donny, B. Downs, D. Drake, G. Dromart, A. Dupont, B. Duston, J. Dworkin, M. D. Dyar, L. Edgar, K. Edgett, C. Edwards, L. Edwards, B. Ehmann, B. Ehresmann, J. Eigenbrode, B. Elliott, H. Elliott, R. Ewing, C. Fabre, A. Fairén, K. Farley, J. Farmer, C. Fassett, L. Favot, D. Fay, F. Fedosov, J. Feldman, S. Feldman, M. Fisk, M. Fitzgibbon, M. Floyd, L. Flückiger, O. Forni, A. Fraeman, R. Francis, P. François, C. Freissinet, K. L. French, J. Frydenvang, A. Gaboriaud, M. Gailhanou, J. Garvin, O. Gasnault, C. Geffroy, R. Gellert, M. Genzer, D. Glavin, A. Godber, F. Goesmann, W. Goetz, D. Golovin, F. Gómez Gómez, J. Gómez-Elvira, B. Gondet, S. Gordon, S. Gorevan, J. Grant, J. Griffes, D. Grinspoon, J. Grotzinger, P. Guillermot, J. Guo, S. Gupta, S. Guzewich, R. Haberle, D. Halleaux, B. Hallet, V. Hamilton, C. Hardgrove, D. Harker, D. Harpold, A. M. Harri, K. Harshman, D. Hassler, H. Haukka, A. Hayes, K. Herkenhoff, P. Herrera, S. Hettrich, E. Heydari, V. Hipkin, T. Hoehler, J. Hollingsworth, J. Hudgins, W. Huntress, J. Huowitz, S. Hviid, K. Iagnemma, S. Indyk, G. Israël, R. Jackson, S. Jacob, B. Jakovsky, E. Jensen, J. K. Jensen, J. Johnson, M. Johnson, S. Johnstone, A. Jones, J. Joseph, I. Jun, L. Kah, H. Kahampää, M. Kahre, N. Karpushkina, W. Kasprzak, J. Kauhanen, L. Keely, O. Kemppinen, D. Keymeulen, M. H. Kim, K. Kinch, P. King, L. Kirkland, G. Kocurek, A. Koefoed, J. Köhler, O. Kortmann, A. Kozyrev, J. Krezowski, D. Krysak, R. Kuzmin, J. L. Lacour, V. Lafaille, Y. Langevin, N. Lanza, J. Lasue, S. Le Mouélic, E. M. Lee, Q. M. Lee, D. Lees, M. Lefavor, M. Lemmon, A. Lepinette Malvitte, R. Léveillé, É. Lewin-Carpintier, K. Lewis, S. Li, L. Lipkaman, C. Little, M. Litvak, E. Lorigny, G. Lugmair, A. Lundberg, E. Lyness, M. Madsen, J. Maki, A. Malakhov, C. Malespin, M. Malin, N. Mangold, G. Manhes, H. Manning, G. Marchand, M. Marín Jiménez, C. Martín García, D. Martin, M. Martin, J. Martínez-Frías, J. Martín-Soler, F. J. Martín-Torres, P. Mauchien, S. Maurice, A. McAdam, E. McCartney, T. McConnochie, E. McCullough, I. McEwan, C. McKay, S. McLennan, S. McNair, N. Melikechi, P. Y. Meslin, M. Meyer, A. Mezzacappa, H. Miller, K. Miller, R. Milliken, D. Ming, M. Minitti, M. Mischna, I. Mitrofanov, J. Moersch, M. Mokrousov, A. Molina Jurado, J. Moores, L. Mora-Sotomayor, J. M. Morookian, R. Morris, S. Morrison, R. Mueller-Mellin, J. P. Muller, G. Muñoz Caro, M. Nachon, S. Navarro López, R. Navarro-González, K. Nealson, A. Neftyan, T. Nelson, M. Newcombe, C. Newman, H. Newsom, S. Nikiforov, B. Nixon, E. Noe Dobrea, T. Nolan, D. Oehler, A. Ollila, T. Olson, M. Á. de Pablo Hernández, A. Paillet, E. Pallier, M. Palucus, T. Parker, Y. Parot, K. Patel, M. Paton, G. Paulsen, A. Pavlov, B. Pavri, V. Peinado-González, L. Peret, R. Perez, G. Perrett, J. Peterson, C. Pilorget, P. Pinet, J. Pla-García, I. Plante, F. Poitrasson, J. Polkko, R. Popa, L. Posiolova, A. Posner, I. Pradler, B. Prats, V. Prokhorov, S. W. Purdy, E. Raaen, L. Radziemski, S. Rafkin, M. Ramos, E. Rampe, F. Raulin, M. Ravine, G. Reitz, N. Rennó, M. Rice, M. Richardson, F. Robert, K. Robertson, J. A. Rodriguez Manfredi, J. J. Romeral-Planelló, S. Rowland, D. Rubin, M. Saccoccia, A. Salamon, J. Sandoval, A. Sanin, S. A. Sans Fuentes, L. Saper, P. Sarrasin, V. Sautter, H. Savijärvi, J. Schieber, M. Schmidt, W. Schmidt, D. Scholes, M. Schopfers, S. Schröder, S. Schwenzer, E. Sebastian Martinez, A. Sengstacken, R. Shterts, K. Siebach, T. Siili, J. Simmonds, J. B. Sirven, S. Slavney, R. Sletten, M. Smith, P. Sobrón Sánchez, N. Spanovich, J. Spray, S. Squyres, K. Stack, F. Stalport, T. Stein, N. Stewart, S. L. Stipp, K. Stoiber, E. Stolper, B. Sucharski, R. Sullivan, R. Summons, D. Sumner, V. Sun, K. Supulver, B. Sutter, C. Szopa, F. Tan, C. Tate, S. Teinturier, I. ten Kate, P. Thomas, L. Thompson, R. Tokar, M. Toplis, J. Torres Redondo, M. Trainer, A. Treiman, V. Tretyakov, R. Urqui-O’Callaghan, J. Van Beek, T. Van Beek, S. VanBommel, D. Vaniman, A. Varenikov, A. Vasavada, P. Vasconcelos, E. Vicenzi, A. Vostrukhin, M. Voytek, M. Wadhwa, J. Ward, E. Weigle, D. Wellington, F. Westall, R. C. Wiens, M. B. Wilhelm, A. Williams, J. Williams, R. Williams, R. B. Williams, M. Wilson, R. Wimmer-Scheingruber, M. Wolff, M. Wong, J. Wray, M. Wu, C. Yana, A. Yen, A. Yingst, C. Zeitlin, R. Zimdar, M. P. Zorzano Mier; MSL Science Team, Isotope ratios of H, C, and O in CO₂ and H₂O of the martian atmosphere. *Science* **341**, 260–263 (2013). [Medline doi:10.1126/science.1237961](https://doi.org/10.1126/science.1237961)
- T. Owen, J. P. Maillard, C. de Bergh, B. L. Lutz, Deuterium on Mars: The abundance of HDO and the value of D/H. *Science* **240**, 1767 (1988). [Medline doi:10.1126/science.240.4860.1767](https://doi.org/10.1126/science.240.4860.1767)
- G. L. Bjoraker, M. J. Mumma, H. P. Larson, Isotopic abundance ratios for hydrogen and oxygen in the martian atmosphere. *Bull. Am. Astron. Soc.* **21**, 991 (1989).

14. J. P. Grotzinger, Analysis of surface materials by the Curiosity Mars rover. *Science* **341**, 1475 (2013). [Medline doi:10.1126/science.1244258](#)
15. G. L. Villanueva, M. J. Mumma, R. E. Novak, Y. L. Radeva, H. U. Käufl, A. Smette, A. Tokunaga, A. Khayat, T. Encrenaz, P. Hartogh, A sensitive search for organics (CH_4 , CH_3OH , H_2CO , C_2H_6 , C_2H_2 , C_2H_4), hydroperoxyxl (HO_2), nitrogen compounds (N_2O , NH_3 , HCN) and chlorine species (HCl , CH_3Cl) on Mars using ground-based high-resolution infrared spectroscopy. *Icarus* **223**, 11–27 (2013). [doi:10.1016/j.icarus.2012.11.013](#)
16. J.-P. Bibring, Y. Langevin, J. F. Mustard, F. Poulet, R. Arvidson, A. Gendrin, B. Gondet, N. Mangold, P. Pinet, F. Forget, M. Berthé, J. P. Bibring, A. Gendrin, C. Gomez, B. Gondet, D. Jouget, F. Poulet, A. Soufflot, M. Vincendon, M. Combes, P. Drossart, T. Encrenaz, T. Fouchet, R. Merchiorri, G. Bellucci, F. Altieri, V. Formisano, F. Capaccioni, P. Cerroni, A. Coradini, S. Fonti, O. Koralev, V. Kottsov, N. Ignatiev, V. Moroz, D. Titov, L. Zasova, D. Loiseau, N. Mangold, P. Pinet, S. Douté, B. Schmitt, C. Sotin, E. Hauber, H. Hoffmann, R. Jaumann, U. Keller, R. Arvidson, J. F. Mustard, T. Duxbury, F. Forget, G. Neukum, Global mineralogical and aqueous Mars history derived from OMEGA/Mars Express data. *Science* **312**, 400–404 (2006). [Medline doi:10.1126/science.1122659](#)
17. M. H. Carr, Retention of an atmosphere on early Mars. *J. Geophys. Res. Planets* **104** (E9), 21897–21910 (1999). [doi:10.1029/1999JE001048](#)
18. W. C. Feldman, T. H. Prettyman, S. Maurice, J. J. Plaut, D. L. Bish, D. T. Vaniman, M. T. Mellon, A. E. Metzger, S. W. Squyres, S. Karunatillake, W. V. Boynton, R. C. Elphic, H. O. Funsten, D. J. Lawrence, R. L. Tokar, Global distribution of near-surface hydrogen on Mars. *J. Geophys. Res. Planets* **109**, E09006 (2004). [doi:10.1029/2003JE002160](#)
19. M. T. Zuber, D. E. Smith, S. C. Solomon, J. B. Abshire, R. S. Afzal, O. Aharonson, K. Fishbaugh, P. G. Ford, H. V. Frey, J. B. Garvin, J. W. Head, A. B. Ivanov, C. L. Johnson, D. O. Muhleman, G. A. Neumann, G. H. Pettengill, R. J. Phillips, X. Sun, H. J. Zwally, W. B. Banerdt, T. C. Duxbury, Observations of the north polar region of Mars from the Mars orbiter laser altimeter. *Science* **282**, 2053–2060 (1998). [Medline doi:10.1126/science.282.5396.2053](#)
20. J. J. Plaut, G. Picardi, A. Safaeinili, A. B. Ivanov, S. M. Milkovich, A. Cicchetti, W. Kofman, J. Mouginot, W. M. Farrell, R. J. Phillips, S. M. Clifford, A. Frigeri, R. Orosei, C. Federico, I. P. Williams, D. A. Gurnett, E. Nielsen, T. Hagfors, E. Heggy, E. R. Stofan, D. Plettemeier, T. R. Watters, C. J. Leuschen, P. Edenhofer, Subsurface radar sounding of the south polar layered deposits of Mars. *Science* **316**, 92–95 (2007). [Medline doi:10.1126/science.1139672](#)
21. M. D. Smith, The annual cycle of water vapor on Mars as observed by the Thermal Emission Spectrometer. *J. Geophys. Res. Planets* **107**, 5115 (2002). [doi:10.1029/2001JE001522](#)
22. T. Fouchet, E. Lellouch, N. I. Ignatiev, F. Forget, D. V. Titov, M. Tschimmel, F. Montmessin, V. Formisano, M. Giuranna, A. Maturilli, T. Encrenaz, Martian water vapor: Mars Express PFS/LW observations. *Icarus* **190**, 32–49 (2007). [doi:10.1016/j.icarus.2007.03.003](#)
23. T. Fouchet, E. Lellouch, Vapor pressure isotope fractionation effects in planetary atmospheres: Application to deuterium. *Icarus* **144**, 114–123 (2000). [doi:10.1006/icar.1999.6264](#)
24. F. Montmessin, T. Fouchet, F. Forget, Modeling the annual cycle of HDO in the martian atmosphere. *J. Geophys. Res. Planets* **110**, E03006 (2005). [doi:10.1029/2004JE002357](#)
25. M. C. Malin, B. A. Cantor, M. R. Wu, L. M. Saper, MRO MARCI Weather Reports (2014) (available at http://www.msss.com/msss_images/subject/weather_reports.html).
26. J. Jouzel, L. Merlivat, Deuterium and oxygen 18 in precipitation: Modeling of the isotopic effects during snow formation. *J. Geophys. Res. Atmos.* **89** (D7), 11749 (1984). [doi:10.1029/JD089iD07p11749](#)
27. J. Laskar, A. C. M. Correia, M. Gastineau, F. Joutel, B. Levrard, P. Robutel, Long term evolution and chaotic diffusion of the insolation quantities of Mars. *Icarus* **170**, 343–364 (2004). [doi:10.1016/j.icarus.2004.04.005](#)
28. J. B. Murray, J. P. Muller, G. Neukum, S. C. Werner, S. van Gasselt, E. Hauber, W. J. Markiewicz, J. W. Head 3rd, B. H. Foing, D. Page, K. L. Mitchell, G. Portyankina; HRSC Co-Investigator Team, Evidence from the Mars Express High Resolution Stereo Camera for a frozen sea close to Mars' equator. *Nature* **434**, 352–356 (2005). [Medline](#)
29. D. P. Page, M. R. Balme, M. M. Grady, Dating martian climate change. *Icarus* **203**, 376–389 (2009). [doi:10.1016/j.icarus.2009.05.012](#)
30. P. H. Smith, L. K. Tamppari, R. E. Arvidson, D. Bass, D. Blaney, W. V. Boynton, A. Carswell, D. C. Catling, B. C. Clark, T. Duck, E. DeJong, D. Fisher, W. Goetz, H. P. Gunnlaugsson, M. H. Hecht, V. Hipkin, J. Hoffman, S. F. Hviid, H. U. Keller, S. P. Kounaves, C. F. Lange, M. T. Lemmon, M. B. Madsen, W. J. Markiewicz, J. Marshall, C. P. McKay, M. T. Mellon, D. W. Ming, R. V. Morris, W. T. Pike, N. Renno, U. Staufer, C. Stoker, P. Taylor, J. A. Whiteway, A. P. Zent, H_2O at the Phoenix landing site. *Science* **325**, 58–61 (2009). [Medline](#)
31. W. V. Boynton, W. C. Feldman, S. W. Squyres, T. H. Prettyman, J. Bruckner, L. G. Evans, R. C. Reedy, R. Starr, J. R. Arnold, D. M. Drake, P. A. Englert, A. E. Metzger, I. Mitrofanov, J. I. Trombka, C. D'Uston, H. Wanke, O. Gasnault, D. K. Hamara, D. M. Janes, R. L. Marcialis, S. Maurice, I. Mikheeva, G. J. Taylor, R. Tokar, C. Shinohara, Distribution of hydrogen in the near surface of Mars: Evidence for subsurface ice deposits. *Science* **297**, 81–85 (2002). [Medline doi:10.1126/science.1073722](#)
32. H. Kurokawa, M. Sato, M. Ushioda, T. Matsuyama, R. Moriaki, J. M. Dohm, T. Usui, Evolution of water reservoirs on Mars: Constraints from hydrogen isotopes in martian meteorites. *Earth Planet. Sci. Lett.* **394**, 179–185 (2014). [doi:10.1016/j.epsl.2014.03.027](#)
33. J. Lasue, N. Mangold, E. Hauber, S. Clifford, W. Feldman, O. Gasnault, C. Grima, S. Maurice, O. Mousis, Quantitative assessments of the martian hydrosphere. *Space Sci. Rev.* **174**, 155–212 (2013). [doi:10.1007/s11214-012-9946-5](#)
34. V. A. Krasnopolsky, M. J. Mumma, G. R. Gladstone, Detection of atomic deuterium in the upper atmosphere of Mars. *Science* **280**, 1576–1580 (1998). [Medline doi:10.1126/science.280.5369.1576](#)
35. T. Usui, C. M. O. Alexander, J. Wang, J. I. Simon, J. H. Jones, *43rd Lunar and Planetary Science Conference* **43**, 1341 (2012).
36. H. Lammer, Origin and evolution of planetary atmospheres: Implications for habitability. *Springer Briefs in Astronomy* **174**, 113–154 (2012).
37. D. E. Smith, M. T. Zuber, H. V. Frey, J. B. Garvin, J. W. Head, D. O. Muhleman, G. H. Pettengill, R. J. Phillips, S. C. Solomon, H. J. Zwally, W. B. Banerdt, T. C. Duxbury, M. P. Golombek, F. G. Lemoine, G. A. Neumann, D. D. Rowlands, O. Aharonson, P. G. Ford, A. B. Ivanov, C. L. Johnson, P. J. McGovern, J. B. Abshire, R. S. Afzal, X. Sun, Mars Orbiter Laser Altimeter: Experiment summary after the first year of global mapping of Mars. *J. Geophys. Res. Planets* **106** (E10), 23689 (2001). [doi:10.1029/2000JE001364](#)
38. M. H. Carr, J. W. Head, Oceans on Mars: An assessment of the observational evidence and possible fate. *J. Geophys. Res. Planets* **108**, 5042 (2003). [doi:10.1029/2002JE001963](#)
39. N. Z. Docto, C. M. O. D. Alexander, J. Wang, E. Hauri, The sources of water in martian meteorites: Clues from hydrogen isotopes. *Geochim. Cosmochim. Acta* **67**, 3971–3989 (2003). [doi:10.1016/S0016-7037\(03\)00234-5](#)
40. J. P. Greenwood, S. Itoh, N. Sakamoto, E. P. Vicenzi, H. Yurimoto, Hydrogen isotope evidence for loss of water from Mars through time. *Geophys. Res. Lett.* **35**, L05203 (2008). [doi:10.1029/2007GL032721](#)
41. P. R. Mahaffy, C. R. Webster, J. C. Stern, A. E. Brunner, S. K. Atreya, P. G. Conrad, S. Domagal-Goldman, J. L. Eigenbrode, G. J. Flesch, L. E. Christensen, H. B. Franz, C. Freissinet, D. P. Glavin, J. P. Grotzinger, J. H. Jones, L. A. Leshin, C. Malespin, A. C. McAdam, D. W. Ming, R. Navarro-Gonzalez, P. B. Niles, T. Owen, A. A. Pavlov, A. Steele, M. G. Trainer, K. H. Williford, J. J. Wray; MSL Science Team, The imprint of atmospheric evolution in the D/H of Hesperian clay minerals on Mars. *Science* **347**, 412–414 (2015). [Medline](#)
42. J. Mouginot, A. Pommerol, P. Beck, W. Kofman, S. M. Clifford, Dielectric map of the martian northern hemisphere and the nature of plain filling materials. *Geophys. Res. Lett.* **39**, L02202 (2012). [doi:10.1029/2011GL050286](#)
43. E. Millour et al., *Third International Workshop on The Mars Atmosphere: Modeling and Observations* **1447**, 9029 (2008).
44. R. T. Clancy, A. W. Grossman, D. O. Muhleman, Mapping Mars water vapor with the very large array. *Icarus* **100**, 48–59 (1992). [doi:10.1016/0019-1035\(92\)90017-2](#)
45. M. J. Wolff, M. D. Smith, R. T. Clancy, R. Arvidson, M. Kahre, F. Seelos IV, S. Murchie, H. Savijärvi, Wavelength dependence of dust aerosol single scattering albedo as observed by the Compact Reconnaissance Imaging Spectrometer. *J. Geophys. Res.* **114**, E00D04 (2009). [doi:10.1029/2009JE003350](#)
46. G. L. Villanueva, M. J. Mumma, R. E. Novak, T. Hewagama, Identification of a new band system of isotopic CO₂ near 3.3 μm : Implications for remote sensing of biomarker gases on Mars. *Icarus* **195**, 34–44 (2008). [doi:10.1016/j.icarus.2007.11.014](#)
47. G. L. Villanueva, M. J. Mumma, K. Magee-Sauer, Ethane in planetary and cometary atmospheres: Transmittance and fluorescence models of the ν_7 band at 3.3 μm . *J. Geophys. Res. Planets* **116**, E08012 (2011).

[doi:10.1029/2010JE003794](https://doi.org/10.1029/2010JE003794)

48. M. D. Smith, J. L. Bandfield, P. R. Christensen, Separation of atmospheric and surface spectral features in Mars Global Surveyor Thermal Emission Spectrometer (TES) spectra. *J. Geophys. Res. Planets* **105** (E4), 9589–9608 (2000). [doi:10.1029/1999JE001105](https://doi.org/10.1029/1999JE001105)

ACKNOWLEDGMENTS

We thank the staff of the Very Large Telescope (VLT, runs 83.C-0538 and 92.C-0436), the NASA InfraRed Telescope Facility (IRTF), and the W. M. Keck Observatory for their exceptional support throughout our long Mars observing Programs. G.L.V. acknowledges support from NASA's Planetary Astronomy Program (08 PAST08 0034) and NASA's Planetary Atmospheres Program (08 PATM08 0031). NASA's Planetary Astronomy Program (RTOP 344 32 07) and NASA's Astrobiology Program (RTOP 344 53 51) supported M.J.M. and G.L.V. NSF RUI supported R.E.N. through grant AST 0805540. This work was also supported by a NASA Keck PI Data Award. The authors recognize and acknowledge the very significant cultural role and reverence that the summit of MaunaKea has always had within the indigenous Hawaiian community. We are most fortunate to have the opportunity to conduct observations from this mountain.

SUPPLEMENTARY MATERIALS

www.sciencemag.org/cgi/content/full/science.aaa3630/DC1

Supplementary Text SM-1 to SM-3

Figs. S1 to S8

References (43–48)

November 2014; accepted 6 February 2015

Published online 5 March 2015

10.1126/science.aaa3630

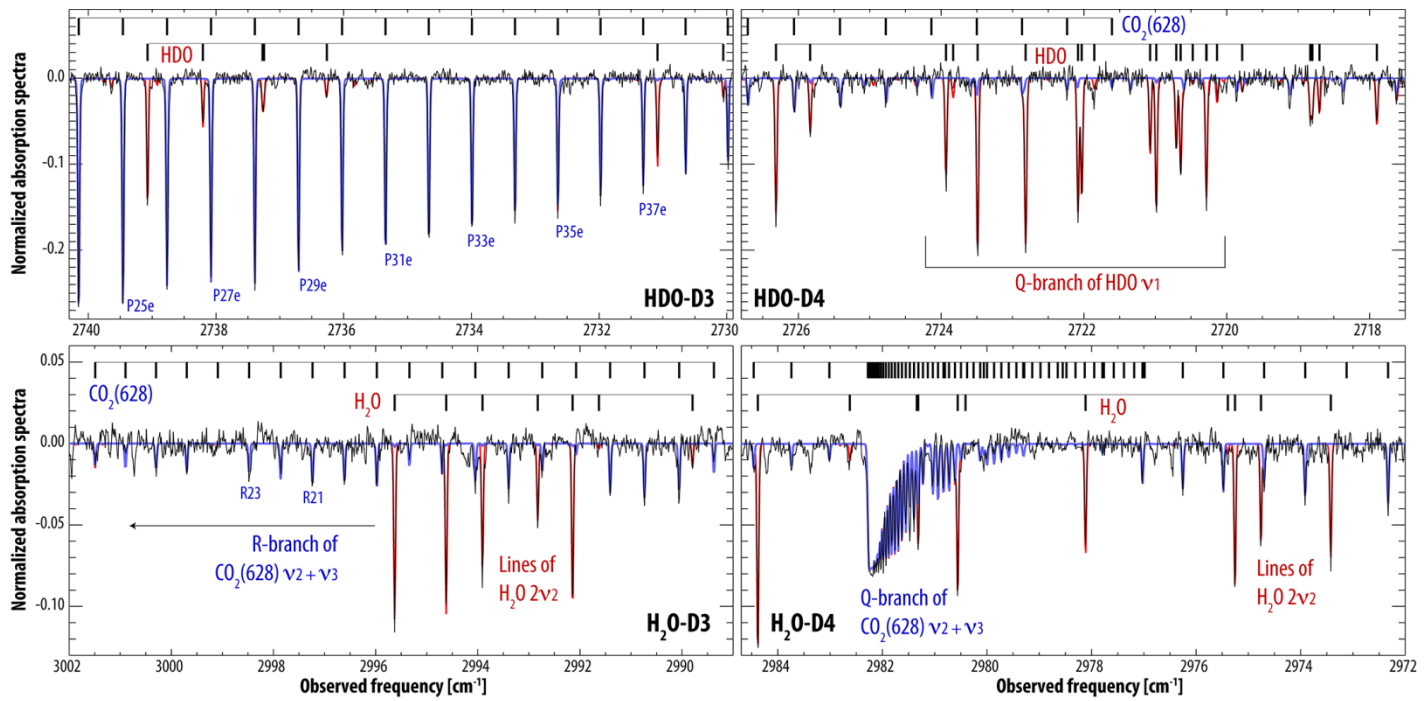


Fig. 1. Mars high-resolution ($\lambda/\delta\lambda \sim 100,000$) residual spectra of HDO, H₂O and CO₂ acquired with two settings of CRIRES at VLT on January 29th 2014 (Ls: 83°). The data shown were extracted for a field-of-view (FOV) 0.2'' (slit width) \times 0.256'' (3 pixels along the slit) over Mars' northern hemisphere (latitude: 57-69°, longitude: 106-133E°). Spectra from detectors D3 and D4 of each CRIRES setting are shown; detectors D1 and D2 reveal additional lines of these species (SM-1). Residual spectral deviation is 0.006 per pixel (1σ). Each martian residual spectrum was derived by subtracting synthetic spectra of the co-measured telluric and solar absorption features (15), after normalizing to the martian continuum. Synthetic models for HDO and H₂O (red trace) and for CO₂ (blue trace) are in good agreement with the measured spectra.

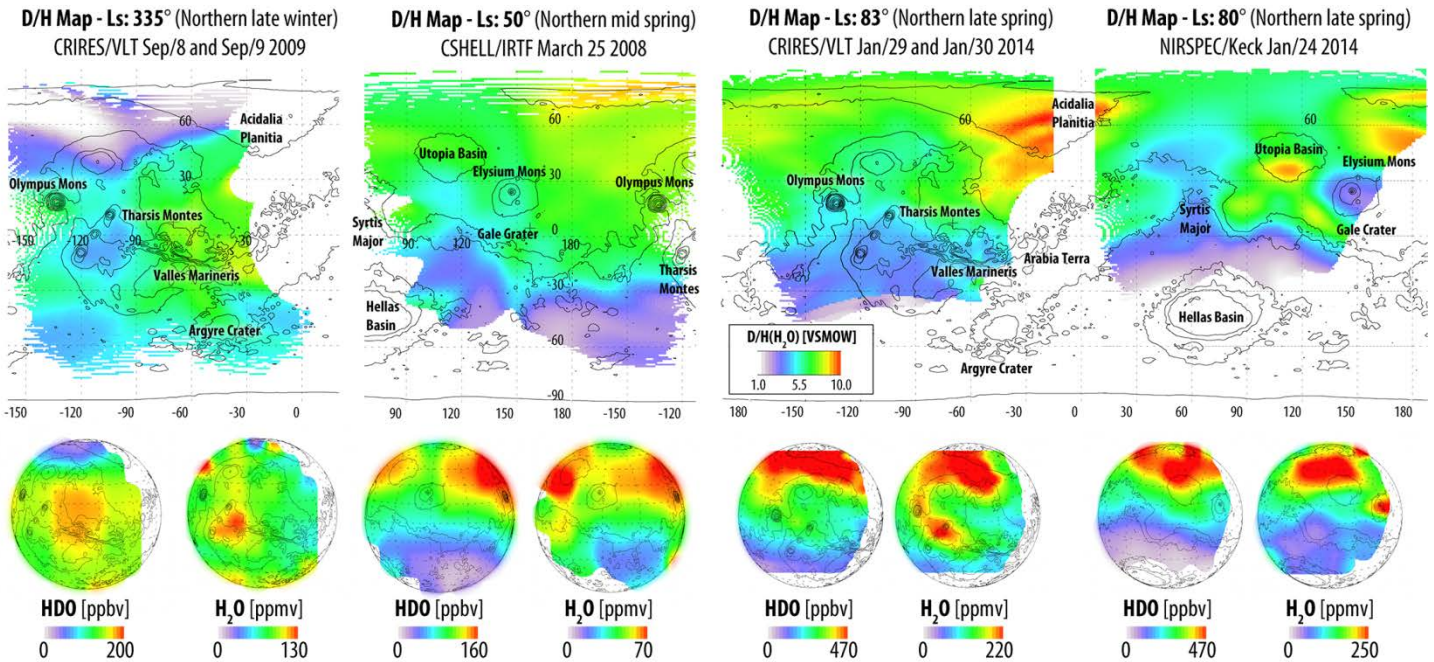


Fig. 2. Maps of deuterated water (HDO) and water (H₂O) and their ratio on Mars, obtained at four different seasons (from late northern winter to late northern spring). D/H maps (upper row) were obtained by ratioing the measured abundance of HDO and H₂O extracted from maps of the individual species (lower row), and are presented relative to the D/H value in Earth's ocean water (VSMOW). The HDO and H₂O data show the progressive enrichment of D/H in the northern hemisphere as the polar cap sublimes during northern spring. The isotopologue disk maps (HDO, H₂O) also reveal strong local enhancements and variability but with significant differences between them, associated with global and local climatology. In particular, low D/H values are observed at regions of low temperature and/or high-altitude, with high values observed at orographic depressions (e.g., Acidalia Planitia, Utopia Basin).

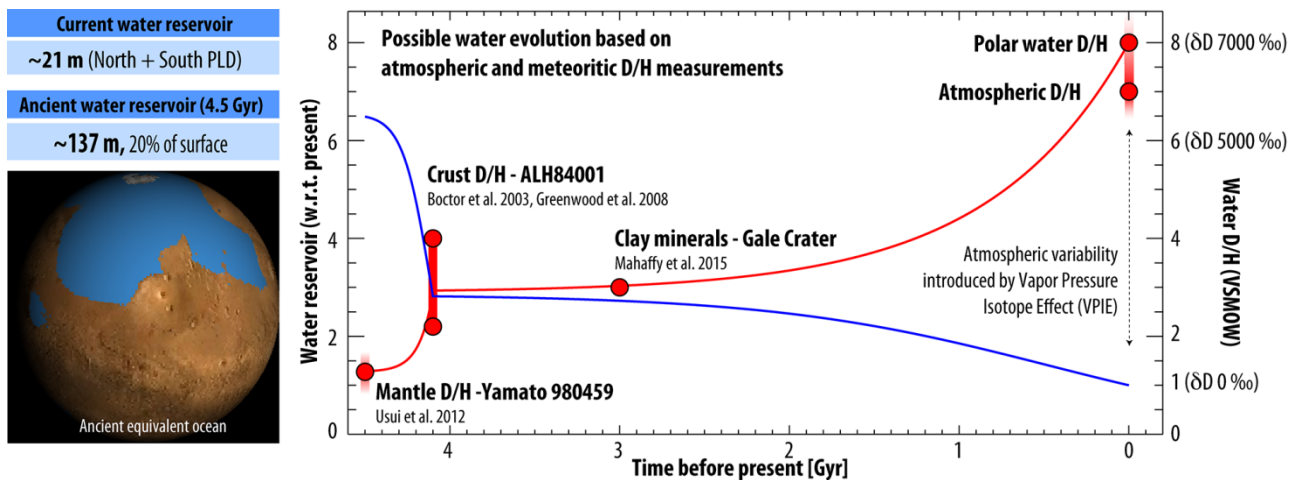


Fig. 3. Isotopic enrichment as evidence for global loss of water on Mars. After correcting for local climatological fractionation of the measured D/H ratio (Fig. 2), the current ratio for D/H in atmospheric water on Mars is at least 7 VSMOW, implying a D/H ratio of 8 VSMOW in the north polar reservoir (red curve and right axis). Assuming a fractionation factor f of 0.02, the D/H ratios obtained from water in Mars meteorites (Yamato 980459, of 4.5 Ga age) imply that Mars' initial water reservoir was larger than the current water available on Mars by a factor of at least 6.5 (blue curve and left axis). When considering the current PLD content of 21 m of water, this would imply that at least 137 m GEL (global equivalent layer) of water was present on Mars 4.5 Ga ago, covering 20% of the planet's surface.